

Evaluation of Static Magnetic Fields Produced by Magnetic Floors Composed of Strontium Ferrite Powder Utilized in the Construction Industry

S. Magdaleno-Adame¹ and Themistoklis D. Kefalas²

¹Magnetic Instrumentation, Indianapolis, IN 46250 USA

²Hellenic Electricity Distribution Network Operator S.A., GR 10434 Athens, Greece

This paper presents a magnetic safety evaluation of the static magnetic field produced by magnetic floors with permanent magnet properties utilized in the construction industry. The magnetic floors analyzed in this paper are composed by a concentration of 85% of isotropic strontium (Sr) ferrite powder mixed with chlorinated polyethylene. The magnetic floors are magnetized and tested in the laboratory to measure the magnetic field levels in different regions of the magnetic floors and magnetic subfloors. Finite-element (FE) simulations are carried out to compute the magnetic field produced by magnetic floors. The numerical results and laboratory tests are compared and analyzed. Values of the magnetic field between 2 and 50 mT are computed and measured in different regions of magnetic floors. Finally, the static magnetic field levels obtained in the magnetic floors are compared with the permitted magnetic field values for different electronic devices, pacemakers, and other common objects utilized by persons in buildings. The results obtained in this paper show that magnetic floors are safe, and they can be employed in buildings without putting in risk electronic devices or persons with pacemakers.

Index Terms— Construction industry, finite-element (FE) simulation, magnetic floor, magnetic resonance imaging (MRI), pacemaker, permanent magnet, strontium ferrite powder.

I. INTRODUCTION

THE magnetic floor technology is being utilized by architects and construction engineers in order to replace the use of convectional floors in different buildings around the world. Magnetic floors present permanent magnet properties which offer great advantages with respect to conventional floors: fast construction times, easy installation, easy to replace, cheap labor costs, resistant to moisture and scratch, and resistant to high-traffic environments. The magnetic floors can be employed in office buildings, mall centers, cinemas, airports, transport stations, apartments, hotels, and so on [1], [2]. The magnetic floors have some disadvantages such as being prone to demagnetization by strong external magnetic fields. For example, the authors do not recommend using magnetic floors in hospital rooms equipped with magnetic resonance imaging scanners which emit magnetic stray fields which could demagnetize the magnetic floors. Moreover, the magnetic floors could experience serious attraction magnetic forces (projectile effect) that could damage them and produce serious safety risk for hospital staff and patients [3].

On the other hand, the architects and construction engineers are skeptical on safety and health issues related with the magnetic field produced by magnetic floors and their effects on persons and electronic devices placed in buildings [4], [5]. There are not official standards in the construction industry to establish the permitted values of static magnetic field produced by magnetic floors, for this reason, it is

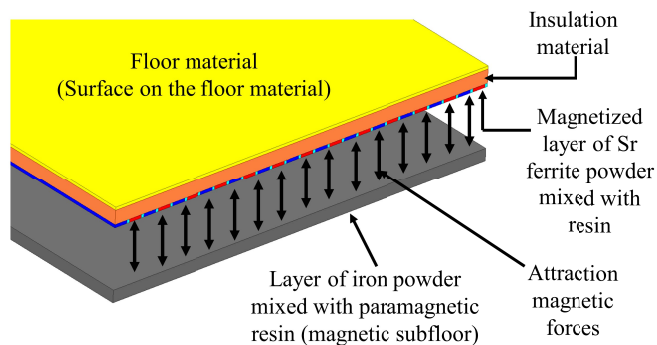


Fig. 1. Magnetic floor equipped with a magnetic subfloor.

important to analyze the static magnetic field produced by magnetic floors to avoid health problems, damaging electronic devices, and other objects in buildings equipped with these floors [4], [5].

The magnetic floors are composed by a magnetic subfloor and a magnetic floor, shown in Fig. 1. A magnetic subfloor consists of a layer of paramagnetic resin mixed with iron powder combined with non-magnetic particles [6]. The average diameter of these iron powder particles is between 50 nm and 500 μm [6]. The paramagnetic resin is composed from 25 to 50 wt% of the epoxy binder, from 50 to 75 wt% of magnetic particles, and with an optional 5wt.% of additive fillers, pigments, extenders, plasticizers, rheology modifiers, thickeners, solvents, tackifiers, and UV-stabilizers [6]. The paramagnetic resin acts as a magnetic material to attract the magnetic floor. On the other hand, a magnetic floor is made of layers of convectional floor material and a layer composed of isotropic strontium (Sr) ferrite powder combined with chlorinated polyethylene [7].

Manuscript received August 4, 2018; revised December 18, 2018; accepted January 18, 2019. Corresponding author: S. Magdaleno-Adame (e-mail: smagdalenoa@hotmail.com).

Color versions of one or more of the figures in this paper are available online at <http://ieeexplore.ieee.org>.

Digital Object Identifier 10.1109/TMAG.2019.2896202

The Sr ferrite powder concentration in magnetic floors is an important manufacturing factor and it should be considered in the production process of magnetic floors. Some authors have studied the effects of Sr ferrite powder concentrations in resins and polymers and other authors analyzed mechanical and magnetic properties of ferrite powders, for example, Stabik *et al.* [8] analyzed low concentrations of Sr ferrite powder (15%–35%) mixed with resins. They noted that the increments of the powder concentrations in the resins increased the remnant magnetization of the magnet powder keeping its coercivity almost constant with small variations. Solomon *et al.* [9] analyzed ceramic Sr ferrite powders mixed with polymers to create rubber ferrite composites. They analyzed different concentrations of Sr ferrite powder (40–120 phr) in polymers and they found that the increments of the Sr ferrite powder concentrations required high magnetic fields to be magnetized. The remnant flux density increased when the powder concentrations are increased while the coercivity of the ferrite powder remained constant. Finally, the authors noted that the increment of ferrite powder concentration increased the hardness of the rubber magnets and reduced the tensile strength and the elongation at break of the rubber magnets. Hosseinpour and Zekery [10] analyzed the magnetic forces produced by Sr ferrite powders and barium ferrite powders with isotropic and anisotropic properties. The authors noted that isotropic Sr ferrite powder produced high magnetic forces compared with the magnetic forces produced by isotropic barium ferrite powders. In addition, the anisotropic Sr ferrite powders produced high magnetic forces compared with isotropic Sr ferrite powders. The magnetic force results obtained in [10] show that Sr ferrite powders should be employed to get excellent magnetic forces in magnetic floors. Lagorce and Allen [11] analyzed different concentrations of anisotropic Sr ferrite powder (50%–80%) mixed with polyimide for micromachining applications. They obtained coercivities of 318 kA/m and remnant flux densities of 0.3 T with concentration of anisotropic Sr ferrite powder of 80%. They noted that Young’s modulus increased with increasing the Sr ferrite powder concentrations. Moreover, the increments of the anisotropic Sr ferrite powder concentrations increased the magnetic field required to magnetize the anisotropic Sr ferrite powder. Furthermore, the magnetic floors should be flexible, easy to install and to replace, and with appropriate and good magnetic forces, for this reason, the magnetic floors are produced using concentrations from 85% to 95% of isotropic Sr ferrite powder with compositions from 5% to 15% of chlorinated polyethylene [7]. On the other hand, the isotropic Sr ferrite powders are utilized in magnetic floors because they are easy to magnetize applying saturation flux densities between 0.3 and 0.5 T [12]–[16]. The magnet powder layer of magnetic floors is magnetized utilizing production machines equipped with magnetic rollers made of neodymium iron boron ring magnets separated by steel rings [17]–[19]. The rollers are utilized to create magnetic striped pole patterns with different numbers of poles per length (in poles per inch) in the magnet powder layer of the magnetic floors [17]–[19]. It is the same process utilized to magnetize flexible magnets (refrigerator magnets) made of Sr ferrite powder [19].

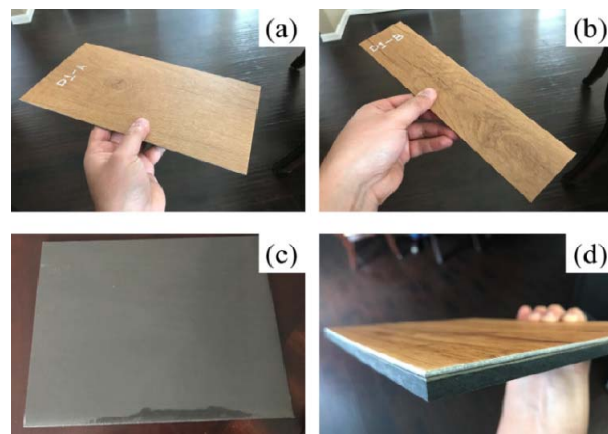


Fig. 2. (a) D1-A magnetic floor. (b) D1-B magnetic floor. (c) Magnetic subfloor (top). (d) Magnetic floor attached to the magnetic subfloor.

The main purpose of this paper is to calculate and to measure the static magnetic fields produced by magnetic floors to determine if the magnetic floor technology is “magnetically” safe for sensitive electronic devices, and for humans with medical devices such as pacemakers. Moreover, an experimental and numerical evaluation of the static magnetic fields produced by actual magnetic floors composed of concentrations of 85% of isotropic Sr ferrite powder is presented. Laboratory tests are carried out to measure the values of the static magnetic field produced by magnetic floors. 2-D finite-element (FE) simulations are performed to compare the results of static magnetic field distributions with the experimental magnetic values. Finally, a magnetic safety analysis is carried out in order to verify and to compare the levels of the static magnetic field produced by magnetic floors with the static magnetic field values permitted by electronic devices, pacemakers, and other objects.

II. LABORATORY MEASUREMENTS

Laboratory tests are carried out to measure the static magnetic field in different regions of a sample of the magnetic floor with and without the presence of the magnetic subfloor. Fig. 2 shows the photographs of the magnetic floors and of the magnetic subfloor utilized in the laboratory tests. The magnetic subfloor is manufactured applying a layer of 1 mm of a commercial gray paramagnetic epoxy resin mixed with magnetic particles on a particle board base with a thickness of 12.7 mm, a length of 279 mm, and a width of 215 mm [3]. Two samples of magnetic floor are tested: D1-A and D1-B, shown in Fig. 2. The D1-B magnetic floor sample has a length of 279 mm and a width $d = 65$ mm. The D1-A magnetic floor sample has a length of 279 mm and a width of 150 mm. The magnetic floor samples have a layer of chlorinated polyethylene mixed with a concentration of 85% of isotropic Sr ferrite powder with an intrinsic coercivity force $H_{ci} = 270$ kA/m and a remnant flux density $B_r = 0.4$ T [7]. The thickness of the layer of Sr ferrite powder mixed with chlorinated polyethylene is of 0.5 mm, the thickness of the floor material is of 0.5 mm, and the thickness of the insulation material is of 2.28 mm.

The magnet powder layer of the magnetic floors is magnetized employing magnetic rollers with ten poles

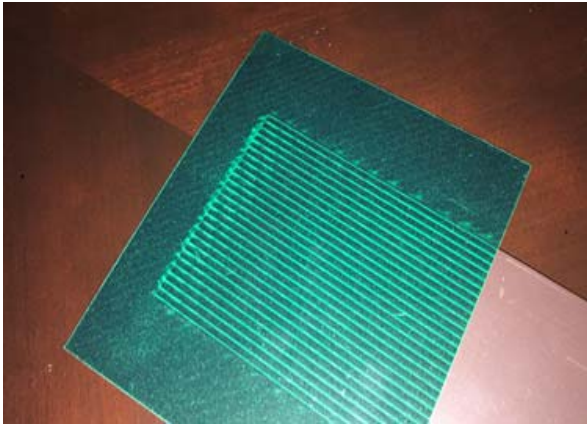


Fig. 3. Photograph of magnetic pole patterns in the magnet powder layer of the D1-B magnetic floor.

per inch (10 PPI). The magnetic pole patterns in the magnetic floor are alternated (south/north/south/north). The 26 magnetic striped pole patterns are created in the magnet layer of the D1-B magnetic floor and 62 magnetic striped pole patterns are created in the D1-A magnetic floor. Fig. 3 shows a photograph of the magnetic striped pole patterns in the D1-B sample of the magnetic floor. A green magnetic view film is employed to visualize the striped pole patterns in the magnetic floor.

An experimental magnetic field mapper manufactured by Magnetic Instrumentation is utilized to measure the magnetic field on the surfaces of the magnetic floor samples. The magnetic field mapper is equipped with a axial probe with a Hall effect sensor with a resolution of $\pm 10 \mu\text{T}$ and a $\pm 0.5 \text{ T}$ full scale to measure magnetic fields produced by permanent magnets. The magnetic fields measured by the mapper are sent to a computer for storage and for data manipulation. The laboratory tests are performed under ambient temperature conditions (where $T = 21 \text{ }^\circ\text{C}$). The magnetic fields are measured at half the length of the magnetic floor samples. The tip of the axial probe is located at a distance of 1.0 mm on the surfaces of the magnetic floors to measure the flux density B_z in the z -axis on the surface of the magnetic floors. Fig. 4 shows the “virtual lines” used to measure the magnetic field on the magnetic floors and the measuring directions for the axial probe of the magnetic field mapper.

The values of B_z are measured on the surfaces of the magnet layer and on the surfaces of the material floor of the magnetic floor samples (D1-A and D1-B). Fig. 5 shows the photographs of the D1-B magnetic floor in the magnetic field mapper during the laboratory tests.

Fig. 6(a) shows the B_z distributions measured for the D1-B magnetic floor on the surface of the floor material without the presence of the magnetic subfloor and Fig. 6(b) shows the B_z distribution measured for the D1-B magnetic floor on its magnet powder layer surface with the magnetic subfloor. Fig. 6(c) shows the B_z distribution measured for the D1-A magnetic floor on its floor material surface without a magnetic subfloor. Maximum flux densities of 2 mT are obtained on the surface of the floor material for both magnetic floor samples and average flux densities of 20 mT are obtained

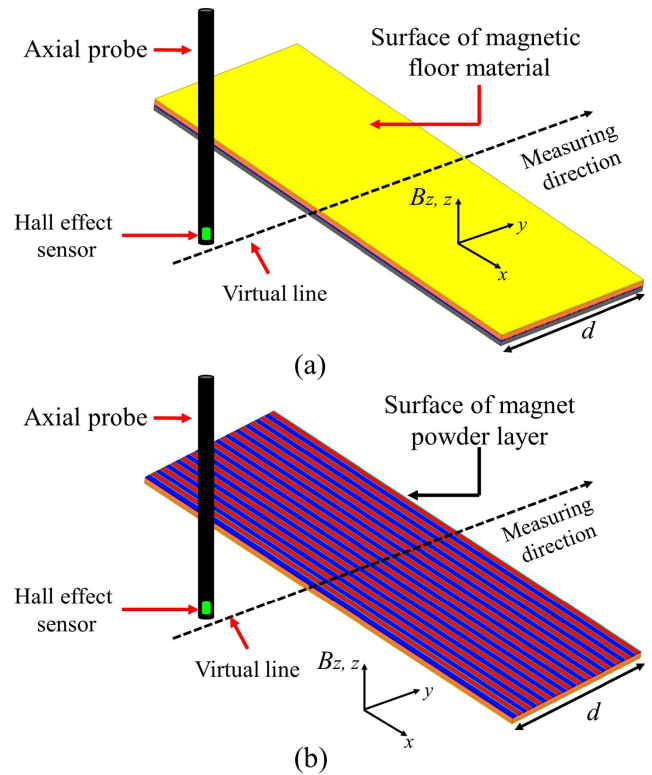


Fig. 4. (a) Virtual line on the floor material of magnetic floor with magnetic subfloor. (b) Virtual line on the magnet powder layer of magnetic floor without magnetic subfloor.

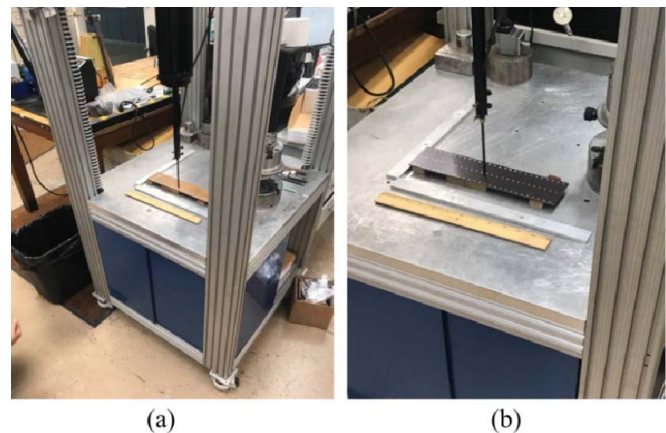


Fig. 5. Photograph of the magnetic field tests on the surface of (a) material floor of D1-B magnetic floor without magnetic subfloor and (b) magnet powder layer of D1-B magnetic floor without magnetic subfloor.

on the surface of the magnet powder layer for both magnetic floor samples without magnetic subfloor. From Fig. 6, one can note that the magnetic field on the surface of the magnet power layer is around ten times higher than the magnetic field on the surface of the floor material of a magnetic floor.

Subsequently, both magnetic floors (D1-A and D1-B) are collocated on the magnetic subfloor and the magnetic field is measured on the floor material surface of the magnetic floors. Fig. 7 shows a photograph of the magnetic floors

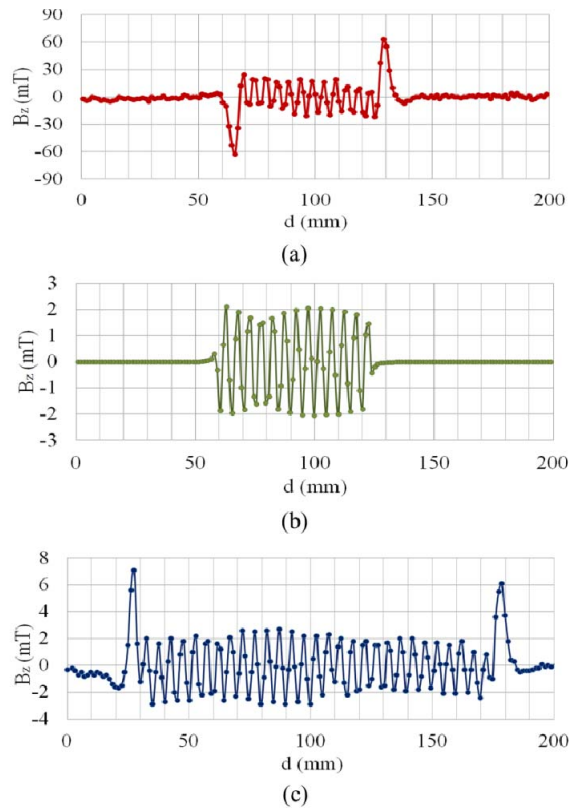


Fig. 6. Magnetic flux density (B_z) measured on (a) magnet powder layer of the D1-B magnetic floor, (b) floor material for the D1-B magnetic floor, and (c) floor material for the D1-A magnetic floor.



Fig. 7. Photograph of the magnetic field test on the surface of magnetic floors (D1-A and D1-B) with the presence of the magnetic subfloor.

(D1-A and D1-B) attached with the magnetic subfloor during the laboratory tests and Fig. 8 shows the flux density B_z distribution measured for the magnetic floors (D1-A and D1-B)

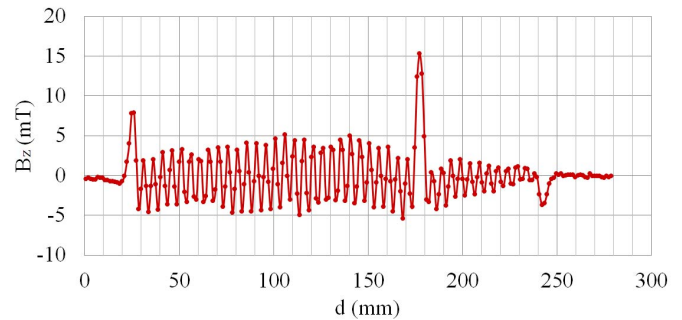


Fig. 8. Magnetic flux density (B_z) measured on the surface of the floor material of magnetic floors (D1-A and D1-B) with the magnetic subfloor.

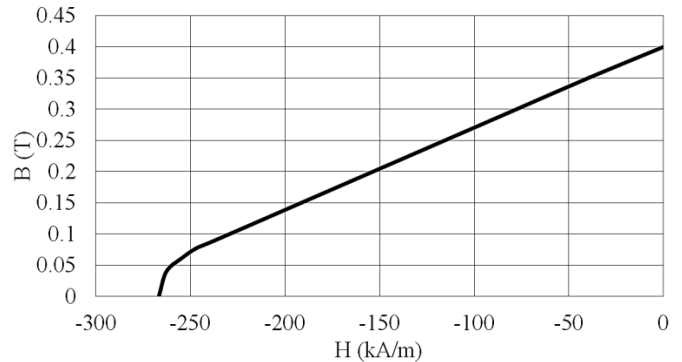


Fig. 9. Demagnetization curve for the magnet powder.

with the magnetic subfloor. Flux densities B_z between 2 and 5 mT are measured on the surface of the floor material of the magnetic floors with the magnetic subfloor. The presence of the magnetic subfloor increases the reluctance of the magnetic floor system and it changes the distribution of magnetic field in the regions of the magnetic floors. As a result, the magnetic flux density on the floor material surfaces is increased (approximately two times) in comparison with the case where the magnetic floors are not attached to the magnetic subfloor.

III. FINITE-ELEMENT SIMULATIONS

The 2-D FE magnetic static analyses are performed to compute the static magnetic field distribution of the magnetic floor sample with and without attached magnetic subfloor sample. ANSYS Maxwell software is employed to compute the magnetic field distributions in magnetic floors using the nonlinear isotropic properties of the Sr ferrite powder.

A. Magnetic Floor Without Magnetic Subfloor

The 26 poles in the magnet layer of the D1-B magnetic floor sample are modeled utilizing north and south sections with a width of 2.286 mm and a thickness of 0.5 mm. The north and south sections of Sr ferrite powder in the magnetic floor are modeled as permanent magnets utilizing the magnetic properties of the Sr ferrite powder. The demagnetization curve of the Sr ferrite powder is utilized in the north and south regions of the magnetic floor. Fig. 9 shows the demagnetization curve for the Sr ferrite powder.

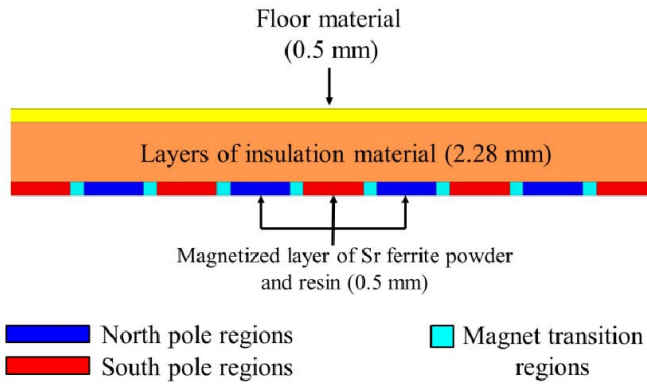


Fig. 10. FE model of magnetic floor without magnetic subfloor.

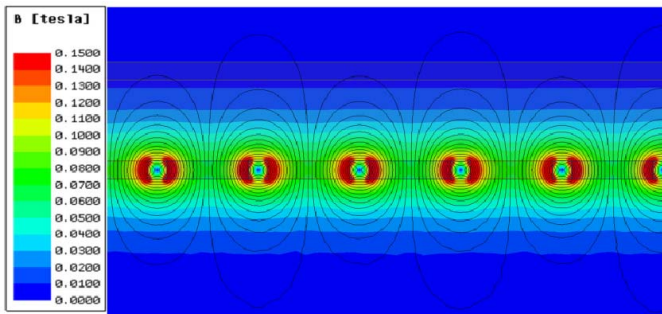


Fig. 11. Magnetic flux density distribution in the magnetic floor region without magnetic subfloor.

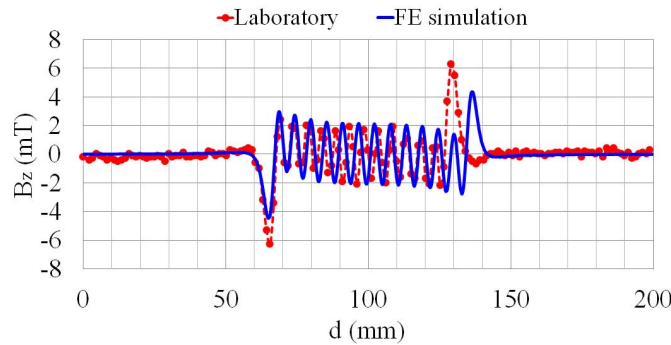


Fig. 12. Comparison between magnetic flux density (B_z) measured and calculated on the surface of the floor material region of the D1-B magnetic floor without magnetic subfloor.

The transition regions between north and south regions are modeled using sections with a width of 0.508 mm and a thickness of 0.5 mm, shown in Fig. 10. These transition regions are modeled as air gaps with a relative permeability $\mu_r = 1$, indicating that these areas are completely saturated after the magnetization of the magnetic floor.

Fig. 11 shows the magnetic flux density distribution in the magnetic floor regions without the presence of the magnetic subfloor, and Fig. 12 shows the comparison between measured and calculated flux densities B_z on the surface of the floor material of the magnetic floor without the magnetic subfloor. In Fig. 12, one can see some differences between the results obtained in the laboratory and in the results obtained in the

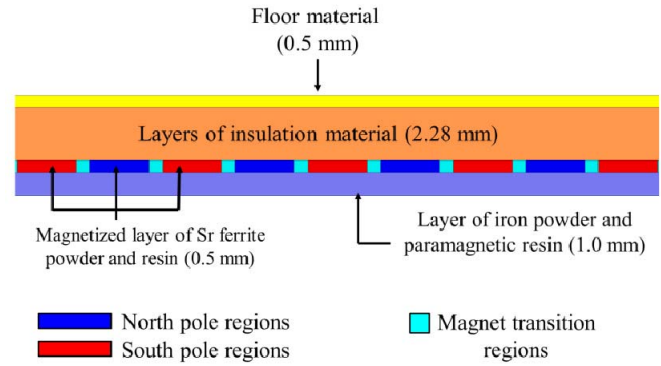


Fig. 13. FE model of magnetic floor with magnetic subfloor.

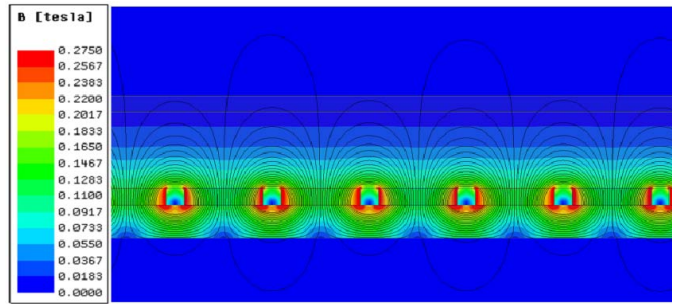


Fig. 14. Magnetic flux density distribution in the magnetic floor region with magnetic subfloor.

FE simulation, especially in the transition regions between north and south regions. The origin of these differences is because of that the ring magnets of the magnetic rollers used to magnetize the magnet powder layers of magnetic floors are not uniformly magnetized, and then, the magnetic rollers produce non-uniform pole patterns in the magnet powder layer of magnetic floors during the magnetization and production process. The magnetization issues, the effects of the joints between adjacent magnetic floors, and other issues present during the production process of magnetic floors are omitted.

B. Magnetic Floor With Magnetic Subfloor

Both magnetic floors D1-A and D1-B are analyzed using FE simulations and compared with the laboratory measurements. The paramagnetic resin of the magnetic subfloor is modeled utilizing a relative permeability $\mu_r = 10$. The thickness of the paramagnetic resin layer is of 1.0 mm as shown in Fig. 13.

Fig. 14 shows the magnetic flux density distribution in the magnetic floor region with the presence of the magnetic subfloor. Fig. 14 also shows that the presence of the magnetic subfloor modifies the paths of the magnetic flux in the magnetic floor region. The paramagnetic resin layer produces a low reluctance path for the magnetic field, and it increases the magnitude of the flux density outside of the magnetic floor. This paramagnetic layer acts as a magnetic shunt for the magnetic floors.

Fig. 15 shows the comparison between the flux densities B_z measured and calculated in the FE simulation on the surface

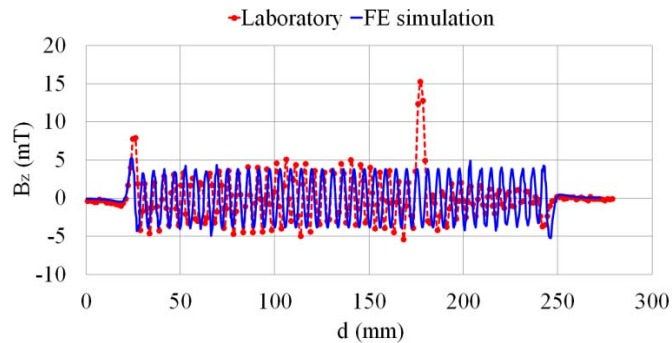


Fig. 15. Comparison between magnetic flux density (B_z) measured and computed on the surface of the floor material region of the D1-A and D1-B magnetic floors with the magnetic subfloor.

TABLE I

PERMITTED VALUES OF STATIC MAGNETIC FIELD FOR ELECTRONIC DEVICES, PACEMAKERS, AND OTHER OBJECTS [20]–[23]

Device	(Static) Magnetic flux density limit level (mT)
New cardiac pacemakers	1.0
Old cardiac pacemakers	0.5
Credit cards	40.0
Magnetic cards	3.0
Mechanical watch	6.0
Hearing aid	20.0

of the floor material of magnetic floors with magnetic subfloor. The results obtained in the FE simulations show a good agreement compared with laboratory test results. With these numerical/experimental results, the authors validated the FE models of the magnetic floors.

IV. MAGNETIC SAFETY EVALUATION OF STATIC MAGNETIC FIELDS PRODUCED BY MAGNETIC FLOORS

The use of magnetic floors in an actual room of a building under real conditions is analyzed in this section. A magnetic safety evaluation is performed to compute the static magnetic fields on the surface of the material floor of magnetic floors with magnetic subfloors. Table I illustrates the permitted values of static flux density for some electronics' devices, for pacemakers, and for other objects [20]–[23]. The permitted flux density values and the values of flux density computed in simulations are analyzed for determining the possibility of negative effects of the use of magnetic floors in buildings.

FE simulations are performed to compute the magnetic flux density at different heights from the surface of the magnetic floors with magnetic subfloors. A room with a surface of 4 m^2 is considered in this paper. The average flux density values are calculated at different heights from the surface of the magnetic floor. Table II shows the average magnetic flux density values computed in the FE simulation for different distances from the surface of the magnetic floor.

From Tables I and II, one can note that the magnetic field produced by magnetic floors cannot damage old and new

TABLE II
AVERAGE MAGNETIC FLUX DENSITY VALUES COMPUTED FOR DIFFERENT DISTANCES OF THE SURFACE OF THE MAGNETIC FLOOR

Device or Condition (Distance on surface of magnetic floor)	Average static magnetic flux density values
Credit cards, magnetic cards, mechanical watches, hearing aids (0 mm)	6 mT
persons with pacemakers lying face down on surface of magnetic floor (50 mm)	$1.23 \mu\text{T}$
persons with pacemakers laying on surface of magnetic floor (200 mm)	$0.26 \mu\text{T}$
(300 mm)	170.00 nT
(500 mm)	86.70 nT
(600 mm)	71.10 nT
(750 mm)	55.10 nT
(1000 mm)	44.10 nT
(1250 mm)	35.30 nT
(1500 mm)	27.60 nT
(2000 mm)	19.20 nT
(2500 mm)	14.80 nT
(3000 mm)	12.00 nT

pacemakers if they are located or put directly on the surface of the magnetic floors. There is a gap between the objects and the surface of the magnetic floor where the flux densities are lower than 6 mT. In addition, persons with old and new pacemakers could not be affected by these magnetic fields if they are lying face down or laying down on the surface of the magnetic floor. Therefore, some magnetic cards and mechanical watches cannot be damaged if they are put directly on the surface of the magnetic floors. Finally, credit cards and hearing aids are not affected by the magnetic fields produced by magnetic floors.

V. CONCLUSION

The results of a numerical and experimental evaluation of static magnetic fields produced by magnetic floors composed of strontium (Sr) ferrite powder are presented in this paper.

Magnetic field measurements are carried out in a laboratory in order to measure the static magnetic field produced by magnetic floors. The results obtained in the laboratory are compared with numerical simulations. Accurate results are obtained between the magnetic fields computed and measured in the laboratory in different regions of the magnetic floors.

Authors calculated and measured static magnetic fields between 4 and 6 mT on the surface of magnetic floors equipped with their magnetic subfloors.

Finally, a magnetic safety analysis is carried out for the magnetic floors. The magnetic fields are computed at different heights from the magnetic floors and they are compared with the permitted magnetic field values for electronic devices, pacemakers, and other objects. Authors concluded that the pacemakers cannot be damaged by magnetic floors if they are collocated directly on the surface of magnetic floors and persons with pacemakers cannot be affected by magnetic floors. In addition, other objects and electronic devices cannot be damaged by magnetic floors.

ACKNOWLEDGMENT

The authors would like to thank Magnetic Instrumentation for its help to carry out the laboratory tests of the magnetic floors. They would also like to thank T. J. Lutz, President of ICT Construction and Technology Corporation, and his engineering team for the magnetic floor and subfloor samples and for the technical information about the magnetic floors.

REFERENCES

- [1] *Intelligent Flooring Systems and IOBAC: Introducing IOBAC Technology*, IOBAC U.K. LTD, London, U.K., 2016, pp. 1–20.
- [2] *IOBAC Magnetised Flooring Technology: A Brand New Concept in Flooring-Adhesive Free for Interface Carpet Tiles and Karndean Design-flooding Luxury Vinyl Tiles*, IOBAC U.K. LTD, U.K., 2018, pp. 1–16.
- [3] *MRI Safety Guidelines Version 2.0*, The Royal Australian and New Zealand College of Radiologists, Druitt St, Sydney, Australia, Dec. 2017, pp. 1–36.
- [4] *Phase 1: Magnetic Flux Density Measurements*, Magnetic Building Solutions, LLC, Dalton, GA, USA, 2017, pp. 1–24.
- [5] *Phase 2: Review of Possible Adverse Health Effects of a Magnetic Flooring System*, Magnetic Building Solutions, LLC, Dalton, GA, USA, 2017, pp. 1–24.
- [6] I. Robinson, W. Jobling, I. Spreadborough, and D. Smyth, “Magnetic floor surface,” U.S. Patent EP 2671853B1, Dec. 12, 2014.
- [7] *Phase 1: Magnetic Safety Data Sheet Rubber Magnet*, Magnetic Building Solutions, LLC, Dalton, GA, USA, 2018, pp. 1–3.
- [8] J. Stabik, A. Chrobak, G. Haneczok, and A. Dybowska, “Magnetic properties of polymer matrix composites filled with ferrite powders,” *Arch. Mater. Sci. Eng.*, vol. 48, no. 2, pp. 97–102, 2011.
- [9] M. A. Soloman, P. Kurian, M. R. Anantharaman, and P. A. Joy, “Evaluation of the magnetic and mechanical properties of rubber ferrite composites containing strontium ferrite,” *Polymer-Plastics Technol. Eng.*, vol. 43, no. 4, pp. 1013–1028, 2004.
- [10] A. Hosseinpour and A. Zakery, “Investigation of magnetic force for barium and strontium ferrites,” *J. Amer. Ceram. Soc.*, vol. 84, no. 5, pp. 1184–1186, 2001.
- [11] L. K. Lagorce and M. G. Allen, “Magnetic and mechanical properties of micromachined strontium ferrite/polyimide composites,” *J. Microelectromech. Syst.*, vol. 6, no. 4, pp. 307–312, Dec. 1997.
- [12] A. Verma, O. P. Pandey, and P. Sharma, “Strontium ferrite permanent magnet—An overview,” *Indian J. Eng. Mater. Sci.*, vol. 7, pp. 364–369, Oct./Dec. 2000.
- [13] M. Kim, K. Lee, M. Choi, and J. Kim, “Magnetic properties and morphologies of synthesized strontium ferrite powders by the molten salt method,” *IEEE Trans. Magn.*, vol. 54, no. 11, Nov. 2011, Art. no. 2103204.
- [14] K. W. Jeon *et al.*, “Synthesis and magnetic properties of aligned strontium ferrite,” *IEEE Trans. Magn.*, vol. 50, no. 6, Jun. 2014, Art. no. 2503004.
- [15] Y. Hui, W. Cheng, G. Lin, and X. Miao, “La-Co pair substituted strontium ferrite films with perpendicular magnetization,” *IEEE Trans. Magn.*, vol. 50, no. 7, Jul. 2014, Art. no. 2800904.
- [16] C. Tanasoiu, P. Nicolau, and C. Miclea, “Preparation and magnetic properties of high coercivity strontium ferrite micropowders obtained by extended wet milling,” *IEEE Trans. Magn.*, vol. MAG-12, no. 6, pp. 980–982, Nov. 1976.
- [17] T. P. Koren, “Portable magnetizer systems,” U.S. Patent 8 174 346 B1, May 8, 2012.
- [18] B. F. Ball, D. W. Rummer, and J. B. Stout, “Material magnetizer systems,” U.S. Patent 8410880B2, Apr. 2, 2013.
- [19] A. J. Olson, C. E. Calderon, P. W. Doolan, E. A. Mengelt, and A. B. Ellis, “Chemistry with refrigerator magnets: From modeling of nanoscale characterization to composite fabrication,” *J. Chem. Educ.*, vol. 76, no. 9, pp. 1205–1211, 1999.
- [20] J. R. Ashley, B. Myers, H. C. Lilly, and R. E. Beatie, “Measurement of potential magnetic field interference with implanted cardioverter defibrillators or pacemakers,” in *Proc. Prof. Program*, Jun. 1998, pp. 159–170.
- [21] *Dental Equipment and Implantable Pacemakers and Defibrillators*, Boston Sci. Corp., Marlborough, MA, USA, Feb. 2009, pp. 1–2.
- [22] R. Beinart and S. Nazarian, “Effects of external electrical and magnetic fields on pacemakers and defibrillators: From engineering principles to clinical practice,” *Circulation*, vol. 128, no. 25, pp. 2799–2809, 2013.
- [23] *Supermagnete Company, What is the Safe Distance That I Need to Keep to my Devices*. Accessed: Nov. 2018. [Online]. Available: <https://www.supermagnete.de/eng/faq>

S. Magdaleno-Adame (M’13) was born in La Piedad de Cavadas, Mexico, in 1983. He received the B.Sc. degree in electrical engineering from the Universidad Michoacana de San Nicolas de Hidalgo, Morelia, Mexico, in 2008, and the M.Sc. degree from the Instituto Tecnológico de Morelia, Morelia, in 2013.

From 2008 to 2010, he was a Research and Development Engineer with Industrias IEM, S.A. de C.V., Tlalhepantla, Mexico. From 2013 to 2014, he was an Electrical Engineer with Pennsylvania Transformer Technology, Canonsburg, PA, USA. From 2015 to 2016, he was a Magnetics Engineer with Correlated Magnetics Research, LCC, Huntsville, AL, USA. From 2017 to 2018, he was a Senior Magnetic and Electromagnetic Engineer with Oersted Technology, Sandy, OR, USA. He is currently an Electromagnetic Engineer with Magnetic Instrumentation, Indianapolis, IN, USA. He has authored over 53 papers. His current research interests include the numerical calculation of electromagnetic and thermal fields in electrical machines, transformers, electromechanical devices, and electromagnetic devices using the finite-element method, combination and application of different magnetic materials in electromagnetic devices, design, and analysis of magnetizing fixtures utilized to produce pulsed high magnetic fields for the magnetization of different magnet materials.

Themistoklis D. Kefalas (M’09) received the Ph.D. degree in electrical and computer engineering and the Ph.D. degree from the National Technical University of Athens, Athens, Greece, in 2005 and 2009, respectively.

From 2010 to 2014, he was an Adjunct Assistant Professor with the School of Pedagogical and Technological Education, Athens, and a Part Time Lecturer with the National Technical University of Athens, Athens, Technological Institute of Piraeus, Aigaleo, Greece, and Technological Institute of Athens, Athens, from 2011 to 2013. From 2005 to 2009, he was with Schneider Electric, Viotia, Greece, where he was involved in distribution transformers. Since 2009, he has been with the National Technical University of Athens, where he is involved in European and National Research Programs concerning the application of electrical machines in the renewable energy market, electricity grids, aerospace industry, and the electric car. Since 2015, he has been with Hellenic Electricity Distribution Network Operator, Athens. He has authored over 23 journal papers and 34 conference papers.

Dr. Kefalas is a member of the Technical Chamber of Greece.